

Achievable Rate with Antenna Size Constraint: Shannon meets Chu and Bode

Volodymyr Shyianov*, Mohamed Akroun*, Faouzi Bellili, *Member, IEEE*,
Amine Mezghani, *Member, IEEE*, Robert W. Heath, *Fellow, IEEE*

Abstract

The achievable rate of existing wireless systems is commonly studied based on mathematical models that disregard the physical limitations of antennas in terms of size, bandwidth, and efficiency. Antenna models are indeed essential to properly analyze the achievable rate as a key performance metric of wireless communication systems. In this work, we use ideas from Chu and Bode/Fano theories to establish the achievable rate under antenna-size constraint. Specifically, we characterize the maximum achievable rate over single-input single-output (SISO) wireless communication channels under a restriction on the antenna size at the receiver. By employing circuit-theoretic multiport models for radio communication systems, we derive the information-theoretic limits of compact antennas. We first describe an equivalent Chu's antenna circuit under the physical realizability conditions of its reflection coefficient. Such a design allows us to subsequently compute the achievable rate for a given size of the receive antenna thereby providing a realistic upper-bound on the system performance that we compare to the standard size-unconstrained Shannon capacity. We also determine the effective signal-to-noise ratio (SNR) which strongly depends on the antenna size and experiences an apparent finite-size performance degradation where only a small fraction of Shannon capacity can be achieved. We further determine the optimal signaling bandwidth which shows that impedance matching is essential in bandwidth-limited scenarios. We also examine the achievable rate in presence of interference showing that the size constraint is immaterial in interference-limited scenarios. Finally, our numerical results of the derived achievable rate as a function of the antenna size and the SNR reveal new insights into concepts for the physical design of radio systems.

Index Terms

Achievable rate, Chu's limit, Size-limited antennas, Impedance Matching.

V. Shyianov, M. Akroun, F. Bellili, and A. Mezghani are with the ECE Department at the University of Manitoba, Winnipeg, MB, Canada (emails: {shyianov, akroutm}@myumanitoba.ca, {Faouzi.Bellili, Amine Mezghani}@umanitoba.ca). R. W. Heath was with The University of Texas at Austin and is now at the North Carolina State University (email: rwheathjr@ncsu.edu). This work was supported by the Natural Sciences and Engineering Research Council of Canada (NSERC) and the US National Science Foundation (NSF) Grant No. ECCS-1711702 and CNS-1731658. *Equal contribution.

I. INTRODUCTION

A. Background and Motivation

The analysis and design of communication systems involve a broad spectrum of scientific disciplines ranging from electromagnetic field theory to communication theory to information theory. The physics of radio communication has been captured in the study of antenna and radio-frequency (RF) engineering. Information theory is an abstract mathematical theory guiding the design and implementation of communication systems. Most of the modern communication theory has evolved around the seminal work of Shannon [1], particularly the capacity of the band-limited AWGN channel. The separation between the physical and mathematical abstractions of communication theory has proved convenient since the two are entirely based on a different set of scientific principles. With many new applications driving the demand for higher frequencies, wider bandwidths, and more compact antennas, it is not possible anymore to keep a clean separation without losing essential insights. Merging the well-established fields of information theory and electromagnetic field theory has led to the development of new paradigms such as the *wave theory of information* [2], *electromagnetic information theory* [3], [4], and *circuit theory for communication* [5]. The variety of studies in wave radiation and propagation systems has shown that circuit and electromagnetic field theories are essential for the analysis and design of multiple-input and multiple-output (MIMO) communication systems [5], [6]. Most of these studies, however, are limited to narrowband communication, and further research is still required to ultimately characterize the physical limitations of wireless systems.

Information theory for MIMO wireless systems is well understood from many perspectives [7]. With the advent of massive MIMO [8], the number of base station antennas was allowed to grow large in multi-user scenarios. With cellular handheld and portable communication devices gaining importance in our everyday life, RF and antenna engineers have focused on designing compact antennas [9]. A limited number of studies though have taken advantage of the realizability constraints from both physics and circuit theory viewpoints to establish physically consistent models for wireless systems [5], [6]. In this context, the effect of mutual coupling on MIMO

arrays has been analyzed in [6] by deriving the mutual information¹ of MIMO systems where the mutual coupling accounts for the radiated power constraint, receive matching network as well as array scattering parameters. In [11], the data rate of a two broadband antenna system was derived, along with its matching network characteristic, while incorporating the broadband matching limitations. A more rigorous approach has been developed in [5] to cover not only the physical model of mutual antenna coupling [6] and the transmit/receive impedance matching [11], but also the physics of signal generation and noise modeling. The circuit models developed in [5] for wireless systems incorporate both the intrinsic noise, originating from the receive amplifiers and the extrinsic noise that is received by the antennas. On the same note, it was shown in [12] that the achievable rate with a sufficiently large antenna array under the total radiated power constraint is mainly limited by the fundamental trade-off between the analog beamforming gain and signal bandwidth. More recently, an information-theoretic methodology for analysis and design of broadband antenna systems was proposed in [13], as opposed to the conventional methodology that relies on frequency-dependent conjugate impedance matching which is infeasible for compact wideband antennas [14]. While the work in [5], [6], [11] combined circuit-based models and the usual information-theoretic models, none of them considered the antenna size as a physical constraint in their respective designs.

For electrically small antennas, the authors of [15] analyzed the fundamental limitations from both antenna theory and broadband matching perspectives by deriving lower bounds on the spectral efficiency of a compact MIMO antenna array inserted inside a sphere.

B. Contributions

We derive the maximum rate achievable on the single-input single-output (SISO) wireless communication channel with a restriction on the size of the antenna at the receiver. Using a physically consistent circuit model of radio communication, we find the maximum mutual information per unit time between the input and output signals of the system under the antenna size constraint. This restriction is incorporated into the circuit model by the use of Chu theory [16]. The mutual information is optimized with respect to the matching network (MN) between

¹James Massey mentioned in [10] an interesting definition of the channel as the part of the system we are “unwilling or unable to change”. In this sense, the antenna should not be regarded as part of the channel but rather as a physical constraint that is under our control to a certain extent. To avoid any confusion we will use the term achievable rate instead of capacity throughout the paper.

the antenna and the low-noise amplifier (LNA). Broadband matching theory [14], [17] is further leveraged to obtain a physically realizable MN. For a given size of the receiver antenna structure, the mutual information is computed and compared to the standard size-unconstrained Shannon capacity. It is found that the received SNR is a strong function of the antenna size and that finite-size performance degradation is most apparent in the low-SNR regime where only a small fraction of Shannon capacity can be achieved. We extend the SISO results to find the mutual information in presence of interference. We show that the finite-size performance degradation vanishes in interference-limited scenarios (when interference dominates amplifier noise). Further, we determine the optimal signaling bandwidth thereby showing that impedance matching is essential in bandwidth-limited scenarios.

C. Paper Organization and Notation

We structure the rest of this paper as follows. In Section II, we introduce the communication model, along with its equivalent channel circuit based on the antenna limitations and broadband matching theory by considering the physical constraints established by using Chu and Bode/Fano theories. In Section III, we derive the achievable rate of the resulting channel model given in the form of a parametric equation involving the antenna-size. We then extend the computation of the achievable rate to the homogeneous interference scenario in Section IV by approximating the interference power density. Finally, in Section V, we solve the parametric equations numerically, from which we draw out concluding remarks in the presence or absence of interference.

The following notation is used in this paper. Given any complex number, $\Re\{\cdot\}$, $\Im\{\cdot\}$, and $\{\cdot\}^*$ return its real part, imaginary part, and complex conjugate, respectively. The statistical expectation and variance are denoted as $\mathbb{E}[\cdot]$ and $\text{Var}[\cdot]$, respectively. We also denote j as the imaginary unit (i.e., $j^2 = -1$) and the symbol \times as the cross product between two vectors. Throughout the paper, c denotes the speed of light in vacuum (i.e., $c \approx 3 \times 10^8$), T is the temperature in Kelvin, k is the wave number, ω is the angular frequency, and $k_b = 1.38 \times 10^{-23} \text{ m}^2 \text{ kg s}^{-2} \text{ K}^{-1}$ is the Boltzmann constant. $\mu = 1.25 \times 10^{-6} \text{ m kg s}^{-2} \text{ A}^{-2}$ and $\epsilon = 8.85 \times 10^{-12} \text{ m}^{-3} \text{ kg}^{-1} \text{ s}^4 \text{ A}^2$ are the permeability and permittivity of vacuum.

II. SYSTEM MODEL

When choosing an appropriate tool for analyzing communication systems, it is essential to consider the interface between information and antenna theories. Applying electromagnetic (EM)

field theory directly to communication problems is a difficult endeavour [5]. A circuit-based model for analyzing communication systems, which is consistent with the governing laws of physics, is relatively much simpler.

A. Circuit model of a communication system

A communication channel can be viewed as a black-box establishing the relationship between the port voltages, $(V_1(f), V_2(f))$, and port currents, $(I_1(f), I_2(f))$, through a symmetric admittance matrix \mathbf{Y}_C as depicted in Fig. 1. When a generator is connected to the port of the transmitting antenna, the current flow on the antenna surface generates an EM field in the space outside the antenna structure (i.e., the generator together with the antenna and the transmission line connecting them). Similarly, the reception of the EM signal impinging on the receive antenna is manifested by a voltage induced on the antenna port and a current flow on the antenna surface. From circuit theory, establishing the relationship between port variables is all that is necessary to consistently model the single-input single-output (SISO) communication channel as an *electrical two-port network*.

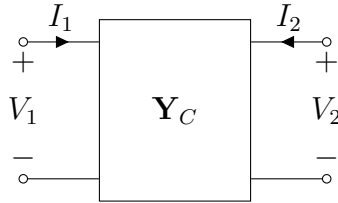


Fig. 1: A communication channel modeled as a two-port network with the channel input port (V_1, I_1) and the channel output port (V_2, I_2)

In information theory, the information-carrying transmitted signals are random processes. From this standpoint, it is insightful to study the mutual information of any physical volume (in space) used for receiving (or generating) these signals. By virtue of their simplicity, circuit-theoretic tools appear to be well suited to such information-theoretic analysis as will be demonstrated later on.

B. Achievable rate of a wireless communication channel

The achievable rate of the continuous-time additive Gaussian noise channel with a certain transmit power spectral density (PSD) $P_t(f)$, a channel frequency response $H(f)$, and a noise

PSD $N(f)$, is given by [18]:

$$C_{\text{bits/s}} = \int_0^\infty \log_2 \left(1 + \frac{P_t(f)|H(f)|^2}{N(f)} \right) df. \quad (1)$$

Taking $|H(f)|^2 = 1$ and $N(f) = N_0$ in (1) yields the well-known capacity of the AWGN channel. In wireless communication, it is more common to include the path-loss in the form of Friis' transmission equation [7]. If d is the distance between the transmitter and receiver and G_t and G_r are receive and transmit antenna gains respectively, the Friis' transmission equation takes the form

$$|H(f)|^2 = G_t G_r \left(\frac{c}{4\pi f d} \right)^2, \quad (2)$$

By the simple application of (2), the signal part of the received power can then be computed from

$$P_r(f) = P_t(f) G_t G_r \left(\frac{c}{4\pi f d} \right)^2. \quad (3)$$

C. The antenna size constraint

Suppose that the receive antenna structure is embedded inside a geometrical spherical volume of radius a . Physical intuition suggests that the data rate should depend on the antenna size, it might be convincing to argue that both the signal and noise powers would be affected in the same way as the antenna size is decreased thereby leaving the SNR, $\text{SNR}(f) = \frac{P_r(f)}{N(f)}$, unchanged. Indeed, while decreasing the antenna size affects the received signal and background radiation noise in the same way, the intrinsic amplifier noise of a realistic receiver would, in turn, make the $\text{SNR}(f)$ or equivalently the achievable rate go to zero. As will be shown in the subsequent sections, the achievable rate in (1) holds approximately only when $W \ll f_c$ where W is the absolute bandwidth of the transmitted signal and f_c is the carrier frequency (in a narrowband system). Although this argument supports the intuition that there should exist a definite relationship between the achievable rate and the receive antenna size, it does not offer a way of obtaining such a relationship. To answer the question of how to find the maximum achievable performance of any antenna structure with a given size, it is necessary to resort to EM field theory. Fortunately, as per Chu's seminal work [16], any antenna structure that can be embedded inside a spherical volume, of a given radius a , can be represented by an equivalent circuit model corresponding to the superposition of TM_n radiation modes. We review in Appendix II Chu's antennas at the detail needed for a comprehensive exposition to their circuit-equivalent representations.

In mobile communication, where isotropic antenna patterns are most preferable, it is enough to consider the first mode of radiation only, i.e., $n = 1$. In this case, the equivalent circuit for the TM_1 wave corresponds to the so-called “*electric Chu’s antenna*” and is illustrated in Fig. 2 which represents its equivalent circuit model at the receiver with

$$V_1 = j \sqrt[4]{\frac{\mu}{\epsilon}} \frac{A_1}{k} \sqrt{\frac{8\pi}{3}} \frac{\partial}{\partial \rho} (\rho h_1(\rho)), \quad (4a)$$

$$I_1 = \sqrt[4]{\frac{\mu}{\epsilon}} \frac{A_1}{k} \sqrt{\frac{8\pi}{3}} \rho h_1(\rho), \quad (4b)$$

$$Z_1 = j \left(\frac{1}{\rho} + \frac{1}{h_1(\rho)} \frac{\partial}{\partial \rho} h_1(\rho) \right). \quad (4c)$$

where $\rho = ka$. Using basic circuit analysis, one can write the input impedance Z_1 as:

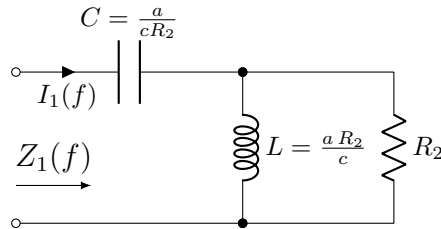


Fig. 2: Equivalent circuit of the TM_1 mode.

$$Z_1 = \underbrace{\frac{1}{j 2\pi f \frac{a}{c}}}_{Z_C} + \underbrace{\frac{1}{\frac{1}{j 2\pi f \frac{a}{c}} + 1}}_{Z_L // Z_R}, \quad (5)$$

which represents the impedance of the circuit illustrated in Fig. 2 with $R_2 = 1$. Note that the circuit properties (4) and (5) of the electric Chu’s antenna are a special case (when $n = 1$) of their general expressions (57) and (59), respectively, for any radiation mode TM_n as reviewed in Appendix II. The antenna structure which excites only the TM_1 mode outside the sphere has the broadest bandwidth², or equivalently the lowest Q-factor, with a linearly polarized omnidirectional pattern [16]. Its Q-factor, namely Q_1 , defined as the ratio between the reactive power, P_{reactive} , and the radiated power, P_{radiated} , is given by

$$Q_1 = \frac{P_{\text{reactive}}}{P_{\text{radiated}}} = \frac{I_1^2(f) \Im\{Z_1\}}{I_1^2(f) \Re\{Z_1\}} = \frac{1}{(ka)^3} + \frac{1}{ka} \quad (6)$$

²A better bandwidth could be achieved (i.e, improved Chu limit) if we combine TM_1 and TE_1 , known as magneto-electric antenna [19], for simplicity consideration is given to the electric antenna only.

The fact that the electric Chu's antenna has the lowest Q-factor compared to all the Chu's antennas operating at higher single modes (i.e. when only one higher mode is excited) allows us to benefit from its desirable broadband property while remaining consistent with the physical constraints of the antenna size. From this perspective, we will rely in this paper on the circuit-theoretic model of the Chu's electric antenna depicted in Fig. 2 to obtain the maximum achievable rate for any radio receiver of a fixed size.

D. Physically realizable impedance matching

It is known that the bandwidth of an antenna can be improved by incorporating an impedance matching network between the antenna and an amplifier. The problem of matching an arbitrary load impedance Z_L to a purely resistive source was addressed in [14]. We review the general principles of broadband matching theory and specialize it to the antenna model at hand in Appendix I. By closely inspecting the circuits in Fig. 4 and 5, the matching problem can be stated with reference to Fig. 3 as follows. Find the conditions of physical realizability of the input impedance, $Z(f)$, or equivalently the input reflection coefficient, $\Gamma(f)$, whose magnitude

$$|\Gamma(f)|^2 = 1 - \frac{P_L(f)}{P_{\max}(f)} \quad (7)$$

corresponds to the fraction of power being rejected by the LNA. Using Darlington representation

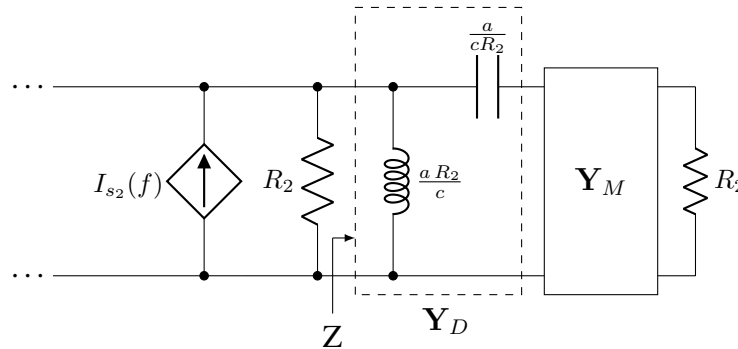


Fig. 3: Matching circuit with Chu antenna.

of Chu-equivalent circuit as we show in Appendix I, the conditions of physical realizability of the reflection coefficient take the form of the following two integral constraints:

$$\frac{1}{2\pi^2} \int_0^\infty f^{-2} \ln \left(\frac{1}{|\Gamma(f)|^2} \right) df = \left(\frac{2a}{c} - 2\gamma^{-1} \right), \quad (8)$$

and

$$\frac{1}{8\pi^4} \int_0^\infty f^{-4} \ln \left(\frac{1}{|\Gamma(f)|^2} \right) df = \left(\frac{4a^3}{3c^3} + \frac{2}{3}\gamma^{-3} \right), \quad (9)$$

where γ is the positive real-valued zero of the reflection coefficient.

We have covered the background on the electric Chu's antenna and its respective optimal transmission coefficient, which will lay the ground for the maximization of the achievable rate of the SISO channel in Section II-F once the SISO channel is fully characterized. This will be covered in the next section.

E. A theoretic-circuit SISO communication model

A circuit-theoretic model of SISO communication systems that includes receive impedance matching, antenna channel and LNA is depicted as in Fig. 4. There, the signal generator is represented by the voltage generator $V(f)$ with its internal resistance R in series. The current sources $I_{N,1}(f)$ and $I_{N,2}(f)$ surrounding the transmit/receive antenna model, \mathbf{Y}_C , account for the extrinsic noise of the transmit antenna and the receive antenna, respectively. In this regard, The conjugate pairs $(V_1(f), I_1(f))$ and $(V_2(f), I_2(f))$ can be interpreted as the voltage and current of the transmit antenna and the receive antenna, respectively. To deliver the maximum power to the load Z_L , the matching network \mathbf{Y}_M matches the input impedance of the receive antenna to the receive amplifier. The equivalent circuit model of the latter framed in a dashed box represents a current amplifier with an input resistance R_{in} that accounts for the fact that the amplifier draws an input current from the matching network, a current-controlled current source, $I_{LNA}(f)$, having a gain factor β in parallel to an independent current source $I_{N,LNA}(f)$ modeling the intrinsic noise of the amplifier [20, chapter 1].

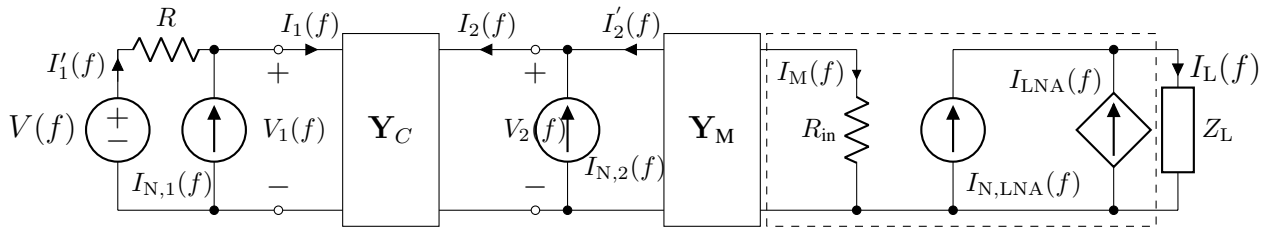


Fig. 4: SISO communication model from left to right: the signal generator $V(f)$ and its resistance R , the extrinsic noise of the transmit antenna $I_{N,1}(f)$, the transmit/receive antenna model \mathbf{Y}_C , the extrinsic noise of the receive antenna $I_{N,2}(f)$, the matching network \mathbf{Y}_M , the receive amplifier model in the dashed box, the load impedance Z_L .

The non-ideal generator voltage, $V(f)$ (i.e. with the internal resistance R) is a frequency-domain representation of the real pass-band signal, $v(t)$, to be transmitted over the channel, i.e.:

$$V(f) = \int_{-\infty}^{+\infty} v(t) e^{-j2\pi ft} dt. \quad (10)$$

As $v(t)$ is a Gaussian random signal, it is convenient to use a Fourier transform truncated to the interval of time T_0 ,

$$V_{T_0}(f) = \int_{-\frac{T_0}{2}}^{+\frac{T_0}{2}} v(t) e^{-2\pi jft} dt, \quad (11)$$

With the definition in (11), the transmit PSD takes the following form:

$$P_t(f) = \lim_{T_0 \rightarrow \infty} \frac{1}{T_0} \frac{\mathbb{E}[|V_{T_0}(f)|^2]}{4R}. \quad (12)$$

Notice that the transmit PSD represents the power that would be radiated by the antenna perfectly matched to the source.

1) *The noisy communication channel model:* The generator terminals are connected to the transmitting antenna through an input port with the current-voltage pair $(I_1(f), V_1(f))$. The channel between the transmit and receive antennas is represented by the frequency-domain admittance matrix \mathbf{Y}_C . The receive antenna terminals are connected to the outside world through the output port with the current-voltage pair $(I_2(f), V_2(f))$. The representation constitutes a noiseless two-port network

$$\begin{bmatrix} I_1(f) \\ I_2(f) \end{bmatrix} = \mathbf{Y}_C \begin{bmatrix} V_1(f) \\ V_2(f) \end{bmatrix}, \quad (13)$$

where the background noise, $(I_{N,1}(f), I_{N,2}(f))$, is injected at both the input and output ports and its second-order moments are determined from [21] once again using truncated Fourier transform:

$$\lim_{T_0 \rightarrow \infty} \frac{1}{T_0} \mathbb{E}[|I_{N,k}(f)|^2] = 4 k_b T \Re\{(\mathbf{Y}_C)_{k,k}\}, \quad k = 1, 2. \quad (14)$$

By applying Kirchhoff's current law (KCL) in Fig. 4, we obtain an affine noisy two-port communication channel

$$\begin{bmatrix} I'_1(f) \\ I'_2(f) \end{bmatrix} = \mathbf{Y}_C \begin{bmatrix} V_1(f) \\ V_2(f) \end{bmatrix} - \begin{bmatrix} I_{N,1}(f) \\ I_{N,2}(f) \end{bmatrix}. \quad (15)$$

The output port of the channel is further connected to the matching network represented by the lossless two-port network with admittance matrix \mathbf{Y}_M . The purpose of the matching network is to assure that the maximum allowable power collected by the antenna gets transferred into the LNA at all frequencies that are present in the signal $V(f)$.

2) *The receive LNA model:* The LNA is modeled at the receiver side as a noisy frequency flat device with gain β as

$$I_{\text{LNA}}(f) = \beta I_{\text{M}}(f). \quad (16)$$

With R_{in} and N_{f} being the input impedance and the noise figure of the amplifier, respectively the second-order statistics of the noise current, $I_{\text{N,LNA}}(f)$, generated inside the LNA are determined using the truncated Fourier transform

$$\lim_{T_0 \rightarrow \infty} \frac{1}{T_0} \mathbb{E}[|I_{\text{N,LNA}}(f)|^2] = \frac{4 k_{\text{b}} T}{R_{\text{in}}} (N_{\text{f}} - 1), \quad (17)$$

The current, $I_{\text{L}}(f)$, flowing into the load impedance, Z_{L} , constitutes the output signal of the communication system.

F. Our proposed achievable rate optimization methodology

To find the maximum achievable rate, it is necessary to optimize the mutual information over the parts of the communication system described above that are at the disposal of the system designer. Once the best possible physically realizable design is identified, the resulting mutual information can be interpreted as a supremum of all achievable rates. By revisiting Fig. 4, it is seen that the transmit waveform, $v(t)$, and the reciprocal lossless matching network, \mathbf{Y}_{M} , are under the full control of the system designer. The channel admittance matrix, \mathbf{Y}_{C} , can also be partially designed by obtaining the optimal transmitter and receiver antenna structures. The maximum mutual information is thus given by:

$$C_{\text{bits/s}} = \max_{\mathbf{Y}_{\text{M}}, \mathbf{Y}_{\text{C}}, \mathbb{P}_v} I(v(t); i_{\text{L}}(t)), \quad (18)$$

where $I(v(t); i_{\text{L}}(t))$ is the mutual information per unit time between the two random processes representing the input and output signals of the communication system [22], [18]. Moreover, \mathbb{P}_v is the probability measure on the space of possible generator voltages, $v(t)$, which for any finite set of time instants $\{t_1, t_2, \dots, t_n\}$ specifies the joint cumulative distribution function:

$$\mathbb{P}_v[v(t_1) \leq v_1, v(t_2) \leq v_2, \dots, v(t_n) \leq v_n] \quad \forall (v_1, v_2, \dots, v_n) \in \mathbb{R}^n. \quad (19)$$

In designing the probability law of the generator, we suppose that the expected per-frequency power constraint, $P_{\text{t}}(f)$, satisfies:

$$P_{\text{t}}(f) \leq E_{\text{max}}, \quad (20)$$

where E_{\max} is the maximum spectral power that the generator is able to supply and is imposed due to regulatory restrictions or hardware constraints.

As explained in Appendix II, the radiation pattern of any antenna structure embedded inside a spherical volume of radius a can be represented by a series of spherical wave functions. Each mode of radiation can then be equivalently characterized by its current-voltage relationship. The equivalent circuit of the antenna which has only the lowest TM_1 mode as the EM field outside the volume is depicted in Fig. 2, where c is the speed of light in vacuum. The antenna gain for this lowest mode in the equatorial plane is $3/2$ [23, chapter 6].

By inspecting Fig. 2, any antenna structure of finite size will necessarily have a reactive component present (associated with non-propagating electromagnetic near-fields) in its input impedance. To seek a maximum radiation efficiency, i.e. a purely resistive input impedance, we take the limit as the size $a \rightarrow \infty$, which renders the capacitance a short circuit and the inductance an open circuit.

In our present investigation, we will focus solely on the size limitation at the receiver side by restricting the volume embodying the transmit antenna to be of infinite size. This leads to the channel model in Fig. 5.

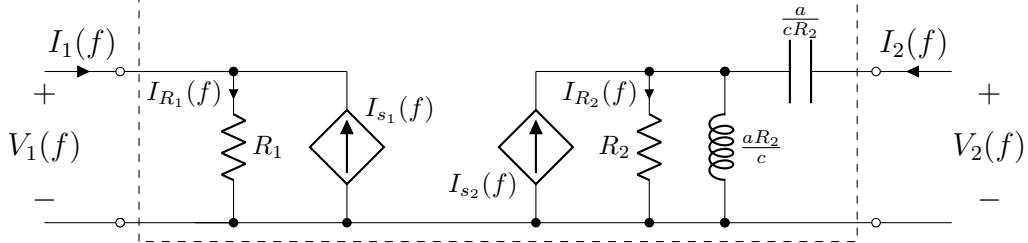


Fig. 5: Channel represented as a two-port network.

From the Friis' equation, we obtain the squared magnitudes of the dependent current sources as:

$$|I_{s_1}(f)|^2 = 4 |I_{R_2}(f)|^2 \left(\frac{c}{4\pi f d} \right)^2 G_r G_t \frac{R_2}{R_1}, \quad (21)$$

and

$$|I_{s_2}(f)|^2 = 4 |I_{R_1}(f)|^2 \left(\frac{c}{4\pi f d} \right)^2 G_r G_t \frac{R_1}{R_2}. \quad (22)$$

From the channel model, the admittance matrix, \mathbf{Y}_C , can be calculated using basic circuit analysis, defining $s = j2\pi f$:

$$\mathbf{Y}_C = \begin{bmatrix} \frac{(saR_2)^2 + (cR_2)^2 + sacR_2^2 - 4\left(\frac{c}{4\pi fd}\right)^2 sacR_2^2 G_t G_r}{((saR_2)^2 + (cR_2)^2 + sacR_2^2)R_1} & \frac{-2cG_t G_r (sa)^2}{4\pi fd((saR_2)^2 + (cR_2)^2 + sacR_2^2)} \sqrt{\frac{R_2^3}{R_1}} \\ \frac{-2cG_t G_r (sa)^2}{4\pi fd((saR_2)^2 + (cR_2)^2 + sacR_2^2)} \sqrt{\frac{R_2^3}{R_1}} & \frac{sa(saR_2 + R_2c)}{(saR_2)^2 + cR_2(saR_2 + R_2c)} \end{bmatrix}. \quad (23)$$

Note here that \mathbf{Y}_C is a symmetric matrix, owing to the reciprocity of antennas. Also, it is common for the signal attenuation between the transmitter and receiver to be extremely large. From the admittance matrix in (23), it can be verified that, in the far-field region (i.e., sufficiently large distance d), $|(\mathbf{Y}_C)_{1,2}| = |(\mathbf{Y}_C)_{2,1}| \ll |(\mathbf{Y}_C)_{1,1}|$. Further, the $(\mathbf{Y}_C)_{1,1}$ entry of the admittance matrix consists of two terms in the numerator with one term being much smaller in magnitude than the other. Consequently, the admittance matrix can be accurately approximated as follows:

$$\mathbf{Y}_C \approx \begin{bmatrix} \frac{1}{R_1} & 0 \\ \frac{-2cG_t G_r (sa)^2}{4\pi fd((saR_2)^2 + (cR_2)^2 + sacR_2^2)} \sqrt{\frac{R_2^3}{R_1}} & \frac{sa(saR_2 + R_2c)}{(saR_2)^2 + cR_2(saR_2 + R_2c)} \end{bmatrix}. \quad (24)$$

The approximate expression in (24) is commonly referred to as the unilateral approximation, that is, the electrical properties at the transmit-side antenna ports are independent of what happens at the receiver. This approximation is an almost exact one for far-field wireless communication systems [5].

In summary, the model for the antenna channel in (24) is the circuit model describing the far-field interaction of two line of sight antennas in which the receiving antenna is constrained to have a maximum size of a meters.

III. COMPUTATION OF THE ACHIEVABLE RATE

In this section, we find the achievable rate in (18) based on the circuit model of SISO communication in Fig. 4 and 5 using the unilateral channel model in (24). Also observing that the noise current, $I_{N,1}(f)$, and the Friis' reaction term, $I_{s_2}(f)$, in (21) are very small compared to the signal current, they can be ignored as part of the unilateral approximation. The goal is to establish the relationship between the real pass-band voltage waveform, $v(t)$, and output current waveform, $i_L(t)$, in (18). First, notice that the output current process $i_L(t)$ can be made Gaussian since the noise sources are Gaussian distributed and all of the circuits are linear. With this, the optimal input voltage process, $v(t)$, must necessarily be a Gaussian random process. We now use a result established in [22] on the mutual information per unit time between two Gaussian random processes to obtain the following result.

Result 1. Let $S_{vv}(f)$, $S_{ii}(f)$, and $S_{vi}(f)$ be continuous spectral and cross-spectral densities of the Gaussian random processes $v(t)$ and $i_L(t)$. Then, the mutual information per unit time between the two Gaussian random processes is given by:

$$\int_0^\infty \log_2 \left(\frac{S_{vv}(f)S_{ii}(f)}{S_{vv}(f)S_{ii}(f) - |S_{vi}(f)|^2} \right) df = \int_0^\infty \log_2 \left(1 + \frac{\beta^2 P_t(f) |H(f)|^2 (1 - |\Gamma(f)|^2)}{\beta^2 N_0 (1 - |\Gamma(f)|^2) + N_{LNA}} \right) df \quad (25)$$

where $N_0 = k_b T$ and $N_{LNA} = k_b T (N_f - 1)$.

Proof. The spectral density of the input process, $v(t)$, is given by $S_{vv}(f) = \lim_{T_0 \rightarrow \infty} \frac{1}{T_0} \mathbb{E}[|V_T(f)|^2]$.

Therefore, (22) becomes:

$$|I_{s_2}(f)|^2 = \frac{S_{vv}(f)}{R R_2} \left(\frac{c}{4\pi f d} \right)^2 G_r G_t, \quad (26)$$

Since the noise is independent of the signal, the PSD of their sum is the sum of their PSDs. By referring to Fig. 3, the PSD of the amplifier current, $I_{mm}(f)$, is given by

$$S_{mm}(f) = \left(\frac{S_{vv}(f)}{R R_2} \left(\frac{c}{4\pi f d} \right)^2 G_r G_t + \frac{4 k_b T}{R_2} \right) (1 - |\Gamma(f)|^2). \quad (27)$$

Hence, the PSD of the output current, $i_L(t)$, is given as the sum of the LNA noise PSD and $\beta^2 S_{mm}(f)$, thereby leading to:

$$S_{ii}(f) = \beta^2 \left(\frac{S_{vv}(f)}{R R_2} \left(\frac{c}{4\pi f d} \right)^2 G_r G_t + \frac{4 k_b T}{R_2} \right) (1 - |\Gamma(f)|^2) + \frac{4 k_b T (N_f - 1)}{R_2}. \quad (28)$$

The final step is to derive the cross-spectral density $S_{vi}(f) = \lim_{T_0 \rightarrow \infty} \frac{1}{T_0} \mathbb{E}[V_T(f) I_L(f)^*]$. First notice that

$$I_{s_2}(f) = V_T(f) \sqrt{\left(\frac{c}{4\pi f d} \right)^2 \frac{G_r G_t}{R R_2}}, \quad (29)$$

and

$$I_L(f) = \beta (I_{s_2}(f) + I_N(f)) A(f) + I_{N,LNA}(f), \quad (30)$$

with $|A(f)|^2 = (1 - |\Gamma(f)|^2)$. Consequently, the cross PSD is given by:

$$S_{vi}(f) = \beta S_{vv}(f) \sqrt{\left(\frac{c}{4\pi f d} \right)^2 \frac{G_r G_t}{R R_2}} A(f), \quad (31)$$

and therefore we have

$$|S_{vi}(f)|^2 = \frac{\beta^2}{2} |S_{vv}(f)|^2 \left(\frac{c}{4\pi f d} \right)^2 \frac{G_r G_t}{R R_2} (1 - |\Gamma(f)|^2). \quad (32)$$

Plugging (28) and (32) back into the left-hand side (25), and recalling the definition in (2) we obtain the desired result. \square

To obtain the maximum achievable rate, we need to maximize the mutual information in (25), over the transmit power spectral density with its constraint in (20), and the reflection coefficient with its two integral constraints in (8) and (9). Notice that since the mutual information is monotonically increasing in the transmit power, then its maximum is achieved by taking $P_t(f) = E_{\max}$. The rest of the optimization problem can be formulated by making the substitution, $\mathcal{T}(f) = |T(f)|^2 = 1 - |\Gamma(f)|^2$, and without loss of generality setting $\beta = 1$ (which is equivalent to divide N_{LNA} by β^2 in (25)), thereby leading to:

$$C_{[b/s]} = \max_{\mathcal{T}(f)} \int_0^\infty \log_2 \left(1 + \frac{E_{\max} |H(f)|^2 \mathcal{T}(f)}{N_0 \mathcal{T}(f) + N_{\text{LNA}}} \right) df \quad (33)$$

$$\text{subject to } \begin{cases} \int_0^\infty f^{-2} \ln \frac{1}{1-\mathcal{T}(f)} df = 2\pi^2 \left(\frac{2a}{c} - 2\gamma^{-1} \right) \triangleq K_1 \\ \int_0^\infty f^{-4} \ln \frac{1}{1-\mathcal{T}(f)} df = 8\pi^4 \left(\frac{4a^3}{3c^3} + \frac{2}{3}\gamma^{-3} \right) \triangleq K_2 \\ 0 \leq \mathcal{T}(f) \leq 1. \end{cases} \quad (34)$$

The Lagrangian associated with (33) and (34) is given by

$$\begin{aligned} J(\mathcal{T}(f)) = & \int_0^\infty \log_2 \left(1 + \frac{E_{\max} |H(f)|^2 \mathcal{T}(f)}{N_0 \mathcal{T}(f) + N_{\text{LNA}}} \right) df \\ & + \mu_1 \left(\int_0^\infty f^{-2} \ln \left(\frac{1}{1-\mathcal{T}(f)} \right) df - K_1 \right) \\ & + \mu_2 \left(\int_0^\infty f^{-4} \ln \left(\frac{1}{1-\mathcal{T}(f)} \right) df - K_2 \right) \\ & + \mu_3 \mathcal{T}(f). \end{aligned}$$

From the gradient condition of variational calculus and complimentary slackness, it follows that:

$$\left. \frac{d}{d\varepsilon} [J(\mathcal{T}^\star(f) + \varepsilon \zeta(f))] \right|_{\varepsilon=0} = 0, \quad (35)$$

for all functions $\zeta(f)$. By taking the derivative in (35) and solving for $\mathcal{T}^\star(f)$ the optimal reflection coefficient is given by the solution of the quadratic equation, by also enforcing the condition that $\mathcal{T}^\star(f)$ must be between zero and one we obtain,

$$\mathcal{T}^\star(f) = \max \left(0, \frac{-C_2(f) - \sqrt{C_2^2(f) - 4C_1(f)C_3(f)}}{2C_1(f)} \right), \quad (36)$$

where

$$C_1(f) = (N_0 + E_{\max}) N_0 (\mu_1 f^{-2} + \mu_2 f^{-4}), \quad (37a)$$

$$C_2(f) = (2 N_0 N_{LNA} + N_{LNA} E_{\max}) (\mu_1 f^{-2} + \mu_2 f^{-4}) - E_{\max} N_f, \quad (37b)$$

$$C_3(f) = E_{\max} N_{LNA} + N_{LNA}^2 (\mu_1 f^{-2} + \mu_2 f^{-4}). \quad (37c)$$

Maximizing the Lagrangian with respect to γ , the optimum is given as:

$$\gamma = 2\pi \sqrt{\frac{\mu_2}{\mu_1}}. \quad (38)$$

Solving the first constraint in (34) for a , we express the antenna size as function of the Lagrange multipliers μ_1 and μ_2 , as follows:

$$a(\mu_1, \mu_2) = \frac{c}{4\pi^2} \int_0^\infty f^{-2} \ln \left(\frac{1}{1 - \mathcal{T}^\star(f)} \right) df + \frac{c}{2\pi} \sqrt{\frac{\mu_1}{\mu_2}}. \quad (39)$$

From the second constraint, we can obtain an implicit relation between the Lagrange multipliers μ_1 and μ_2 :

$$\frac{1}{8\pi^4} \int_0^\infty f^{-4} \ln \left(\frac{1}{1 - \mathcal{T}^\star(f)} \right) df = \frac{4a (\mu_1, \mu_2)^3}{3c^3} + \frac{1}{12\pi^3} \left(\frac{\mu_1}{\mu_2} \right)^{3/2}. \quad (40)$$

Besides, from (40), we can numerically solve for μ_2 for fixed μ_1 which means we need only to specify μ_1 and obtain the antenna size from (39). This is in fact equivalent to fixing the size as well as γ and obtaining the corresponding Lagrange multipliers μ_1 and μ_2 .

We now summarize in Result 3, the main optimization steps obtained in this section.

Result 2. *For a given size of the receiver antenna structure, a , the matched electrical Chu's antenna circuit has the following*

- 1) *An optimal reflection coefficient [cf. (36)]*

$$\mathcal{T}^\star(f) = \max \left(0, \frac{-C_2(f) - \sqrt{C_2^2(f) - 4C_1(f)C_3(f)}}{2C_1} \right),$$

where $C_1(f)$, $C_2(f)$ and $C_3(f)$ are defined in (37).

- 2) *An achievable rate equal to [cf. (33)]*

$$C_{[b/s]} = \int_0^\infty \log_2 \left(1 + \frac{E_{\max} |H(f)|^2 \mathcal{T}^\star(f)}{N_0 \mathcal{T}^\star(f) + N_{LNA}} \right) df. \quad (41)$$

- 3) Two constraints (39) and (40) involving the antenna size, $a(\mu_1, \mu_2)$, as a function of the two Lagrange multipliers μ_1 and μ_2 :

$$a(\mu_1, \mu_2) = \frac{c}{4\pi^2} \int_0^\infty f^{-2} \ln \left(\frac{1}{1 - \mathcal{T}^\star(f)} \right) df + \frac{c}{2\pi} \sqrt{\frac{\mu_1}{\mu_2}},$$

$$\frac{1}{8\pi^4} \int_0^\infty f^{-4} \ln \left(\frac{1}{1 - \mathcal{T}^\star(f)} \right) df = \frac{4a(\mu_1, \mu_2)^3}{3c^3} + \frac{1}{12\pi^3} \left(\frac{\mu_1}{\mu_2} \right)^{3/2}.$$

This result gives the maximum mutual information of a physically realizable antenna of some fixed size a . In fact, any other antenna structure of the same size would be able to achieve mutual information that is strictly smaller than what is given in (41). Our analysis excluded the interference contribution to the received power. In the next section, we consider a different setting where the interference term contribution to the received power is not neglected.

IV. ANALYSIS OF INTERFERENCE

In this section, we extend our model to the homogeneous interference scenario. To produce an analytically tractable model, we leverage tools from stochastic geometry to derive the first two moments of the interference power density. This approach does not require complex computations to estimate the distributions' parameters [24], [25].

We consider a downlink cellular system where the source of interference is a single type of interferer, namely a macrocell of radius R . In this new model, the interferer's locations $x_i \in \mathbb{R}^2$ follow a 2-dimensional Marked Point Process $\Phi = \{x_i, p_i\}$, where the marks $p_i \in \mathbb{R}^+$ correspond to the normalized small-scale channel parameter and follow a unit-mean distribution $\mathbb{P}[p_i \leq s] = G(s)$. Additionally, we consider a Poisson Point Process (PPP) with density ρ such that the marks are exponentially distributed according to the small scale power distribution of the Rayleigh faded channel, i.e. $G(s) = 1 - e^{-s}$. Finally, we also consider an omni-directional path-loss (OPL) function $l(r) = (\frac{r}{\lambda})^\alpha$ as well as Rayleigh small-scale fading for the interference, where α is called the path-loss exponent [26] and guarantees the finiteness of the total interference, i.e., $\alpha > 2$. The intended channel is still assumed to be in line-of-sight condition and thus characterized by Friis' equation.

A. Gamma 2nd Order Moment Matching

Under the model assumptions stated above, the mean and variance of the total received interference power I with Rayleigh fading interference channels are well-known to have the

following expressions [cf. [26]].

$$\mathbb{E}[I] = \frac{2\pi\rho}{\alpha-2} P_t \lambda^\alpha R^{2-\alpha}, \quad (42a)$$

$$\sigma_I^2 \triangleq \text{Var}[I] = 2P_t^2 \frac{\pi\rho}{\alpha-1} \lambda^{2\alpha} R^{2(1-\alpha)}. \quad (42b)$$

Now, given the finite first $\mathbb{E}[I]$ and second order $\mathbb{E}[I^2]$ moments of the interference power I from (42a) and (42b), the characterization of the distribution of the interference power I , $p_I(I)$, can be approximately achieved using the second-order moment matching with the Gamma distribution [27]. The parameters k and θ of the matched Gamma distribution $q_I(I) = \Gamma(I; k, \theta)$ of the interference power I are explicitly given by:

$$k = \frac{\mathbb{E}[I]^2}{\sigma_I^2} = 2\pi\rho R^2 \frac{(\alpha-1)}{(\alpha-2)^2}, \quad (43a)$$

$$\theta = \frac{\sigma_I^2}{\mathbb{E}[I]} = \frac{(\alpha-2)}{(\alpha-1)} P_t \left(\frac{\lambda}{R}\right)^\alpha. \quad (43b)$$

This approximation not only yields a tractable interference distribution but also avoids the need for the Laplace characterizations of (42a) and (42b).

From a circuit perspective, the fact that the interference field of a set of transmitters can be interpreted as a shot-noise field allows us to extend the interference-free model of Fig. 5 to handle the interference scenario. For this reason, we treat the interference term, similarly to the noise term, as an additional independent current source $I_{\text{inter}}(f)$ in parallel to the noise current source $I_{s_2}(f)$.

B. Computation of achievable rate

When the interference I is taken into account, the mutual information (33) with an optimal matching network needs to be slightly modified by augmenting the environmental noise power N_0 with interference power I (i.e $N_0 \Rightarrow N_0 + I$ in (37)). In the presence of interference, the mutual information admits an approximate closed form expression only in case the transmission coefficient $\mathcal{T}(f)$ is known in advance i.e, (a given antenna structure that cannot be adapted to interference). If an antenna is considered to be adaptive, the mutual information does not admit a closed for but can otherwise be found numerically. Notice that in case of interference an optimal Chu's antenna must necessarily be reconfigurable. In other words, the receive antenna should have the capability to adjust its internal matching network circuit such that the transmission coefficient is maximized for every interference realization value.

1) *Mutual information with fixed antenna*: By averaging over the matched interference density $q(I)$, we rewrite the mutual information (33) in this case as follows

$$\begin{aligned} C_{[b/s]} &= \mathbb{E}_{q(I)} \left[\int_0^\infty \log_2 \left(1 + \frac{E_{\max} |H(f)|^2 \mathcal{T}(f)}{(N_0 + I) \mathcal{T}(f) + N_{\text{LNA}}} \right) \mathrm{d}f \right] \\ &= \int_0^\infty \mathbb{E}_{q(I)} \left[\log_2 \left(1 + \frac{E_{\max} |H(f)|^2 \mathcal{T}(f)}{(N_0 + I) \mathcal{T}(f) + N_{\text{LNA}}} \right) \right] \mathrm{d}f. \end{aligned} \quad (44)$$

When the transmission coefficient $\mathcal{T}(f)$ does not depend on the interference I , particularly in the case when the impedance matching is not taken into account, one can set $\mathcal{T}(f)$ to $1 - |\Gamma(f)|^2$ where $\Gamma(f)$ is the derived reflection coefficient (54) in Appendix I.

To derive a closed form to the integrand of (44), we start from the observation that

$$\begin{aligned} \mathbb{E}_{q(I)} \left[\log_2 \left(1 + \frac{E_{\max} |H(f)|^2 \mathcal{T}(f)}{(N_0 + I) \mathcal{T}(f) + N_{\text{LNA}}} \right) \right] &= \mathbb{E}_{q(I)} \left[\log_2 \left((I + N_0 + E_{\max} |H(f)|^2) \mathcal{T}(f) + N_{\text{LNA}} \right) \right] \\ &\quad - \mathbb{E}_{q(I)} \left[\log_2 \left((I + N_0) \mathcal{T}(f) + N_{\text{LNA}} \right) \right]. \end{aligned} \quad (45)$$

By applying the second order Taylor expansion of $f : x \rightarrow \mathbb{E}[\log_2(1 + x)]$ around $\mathbb{E}[x]$, i.e.,

$$\mathbb{E}[\log_2(1 + x)] = \log_2(1 + \mathbb{E}[x]) - \frac{\text{Var}[x]}{2(1 + \mathbb{E}[x])^2} + o(\text{Var}[x]),$$

to the two terms of the right-hand side of (45) separately, we get the following result:

Result 3. *In the homogeneous interference scenario, the approximate closed form expression of the mutual information when the transmission coefficient $\mathcal{T}(f)$ is*

$$\begin{aligned} C_{[b/s]} &= \mathbb{E}_{q(I)} \left[\log_2 \left(1 + \frac{E_{\max} |H(f)|^2 \mathcal{T}(f)}{(N_0 + I) \mathcal{T}(f) + N_{\text{LNA}}} \right) \right] \\ &= \log_2 \left(\frac{((\mathbb{E}[I] + N_0 + E_{\max} |H(f)|^2) \mathcal{T}(f) + N_{\text{LNA}})}{((\mathbb{E}[I] + N_0) \mathcal{T}(f) + N_{\text{LNA}})} \right) \\ &\quad - \frac{\mathcal{T}(f)^2 \sigma_I^2}{2} \left(\frac{((\mathbb{E}[I] + N_0 + E_{\max} |H(f)|^2) \mathcal{T}(f) + N_{\text{LNA}})^{-2}}{((\mathbb{E}[I] + N_0) \mathcal{T}(f) + N_{\text{LNA}})^{-2}} \right) \\ &\quad + o(\sigma_I^2), \end{aligned} \quad (46)$$

where $\mathbb{E}[I]$ and σ_I^2 are the mean and variance of $q(I)$ obtained from (42a) and (42b), respectively. The accuracy of such approximation is high when the last correction term in (46) is much smaller than 1, which corresponds to the condition $\sigma_I^2 \ll \mathbb{E}[I]^2$. The case where the pathloss exponent α is close to 2 would satisfy this requirement.

2) *Mutual information with adaptive antenna and an optimal matching network*: The mutual information (33) is averaged over its matched interference density $q(I)$, i.e.,

$$C_{[b/s]} = \mathbb{E}_{q(I)} \left[\int_0^\infty \log_2 \left(1 + \frac{E_{\max} |H(f)|^2 \mathcal{T}^\star(f)}{(N_0 + I) \mathcal{T}^\star(f) + N_{\text{LNA}}} \right) df \right]. \quad (47)$$

As was mentioned earlier, the mutual information in (47) cannot be found in closed form. In this case, we only compute it numerically (47) in Section V.

Now that we derived the expression of the antenna mutual information under the size constraint with and without considering the interference case, we are ready to compare it to the standard size-unconstrained Shannon limit and examine the effect of the impedance matching as a function of the SNR.

V. NUMERICAL RESULTS AND DISCUSSION

The findings in this section are based on the numerical evaluation of the following expressions

- 1) *Interference-free scenario*: the achievable rate C_a (33) as well as antenna size (39) and physical realizability constraint in (40). The transmission coefficients are given in (36) and (51) with optimal matching and no matching, respectively.
- 2) *Interference scenario*: Under the matched density $q(I)$ of the interference power, we consider the two separate cases:
 - no matching setting: the accurate approximation (46) of the achievable rate $C_{\text{inter}}^{\text{no MN}}$ (44),
 - impedance matching setting: the achievable rate $C_{\text{inter}}^{\text{MN}}$ (47).

We first compare in Fig. 6, the value of the SNR as a function of the frequency:

$$\text{SNR}(f) = \frac{E_{\max} |H(f)|^2 \mathcal{T}(f)}{N_0 \mathcal{T}(f) + N_{\text{LNA}}}, \quad (48)$$

for three different antenna sizes $a \in \{1.05, 1.88, 3.37\}$ cm with both optimal matching network and no matching network in Fig. 6. Referring back to (25), we set the noise figure to $N_f = 2$ (or equivalently 3 dB). The noise temperature $T = 300$ K such that $N_0 = N_{\text{LNA}} = k_b T = 4.14 \times 10^{-21}$ Joules. We also set $d = 1000$ m, $E_{\max} = 1.84 \times 10^{-8}$ Joules, and $G_t = G_r = 3/2$ (TM₁ mode). As see in Fig. 6, a three-fold increase in antenna size leads to approximately ten-fold increase in the SNR. It is also observed that with much larger bandwidth the benefit of matching is rather marginal, although with optimal matching the peak of the SNR shifts to lower frequency as intuitively expected from the Friis' equation.

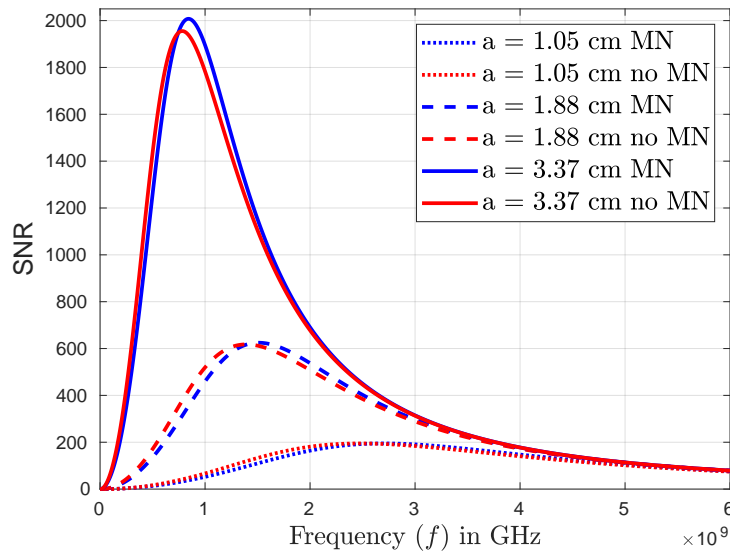


Fig. 6: SNR vs. the frequency (f) for three different antenna sizes a with $E_{\max} = 1.84 \times 10^{-8}$ Joules $N_0 = N_{\text{LNA}} = 4.14 \times 10^{-21}$ Joules and $d = 1000$ m.

In Fig. 7, we plot a fraction of Shannon capacity achievable for a given antenna size. The mutual information C_a is computed from (33) with the optimized transmission coefficient from (36) while the Shannon capacity is determined assuming frequency flat antenna response, i.e.:

$$C_{\text{Shannon}} = \int_0^\infty \log_2 \left(1 + \frac{E_{\max} |H(f)|^2}{N_0 + N_{\text{LNA}}} \right) df. \quad (49)$$

All other parameters are fixed to the same values as in Fig. 6. As was pointed out earlier, Fig. 7 suggests that, at low transmit power density only a small fraction of the total Shannon capacity can be achieved. Note that the achievable fraction is as small as 20% for a one-centimeter antenna. In Fig. 8, we plot the mutual information for four different antenna sizes as a function of the normalized transmit power density with the transmission coefficient being obtained without matching from (51). The parameters $N_0 = N_{\text{LNA}} = 2.07 \times 10^{-21}$ Joules are fixed and the Shannon limit is computed as in (49). In Fig. 9, the transmit power is fixed to $P = 2$ Watts and $E_{\max} = P/W$ is varied while the mutual information is computed from (33). The mutual information is simulated with an antenna size, $a = 0.96$ cm, for the case of no matching (51), optimal matching (36) and frequency flat reflection coefficient in (49). The carrier frequency is fixed to $f_c = 600$ MHz and the bandwidth interval is chosen symmetric around the carrier. It is interesting to notice that the optimal bandwidth is lower for the case of matching while still being a large fraction of the carrier frequency (i.e, broadband system). It should be noted that the carrier frequency could also be optimized for some fixed bandwidth, or even both together.

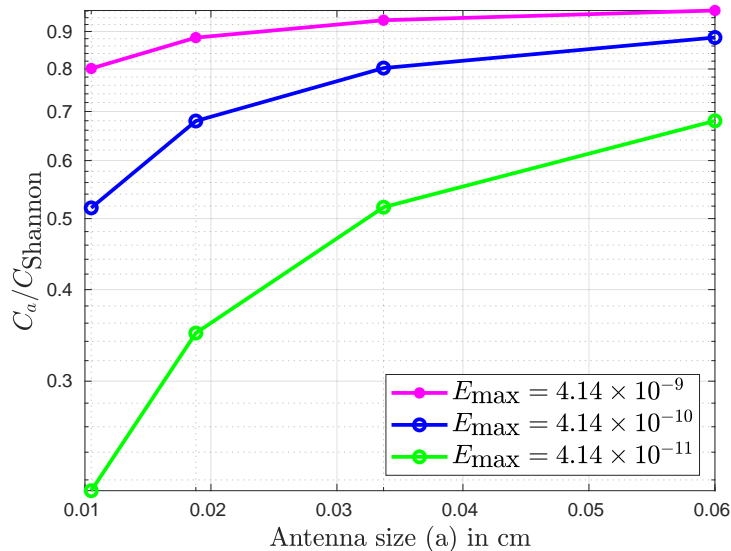


Fig. 7: Achievable fraction of the Shannon capacity vs. the antennas size at three different SNR levels.

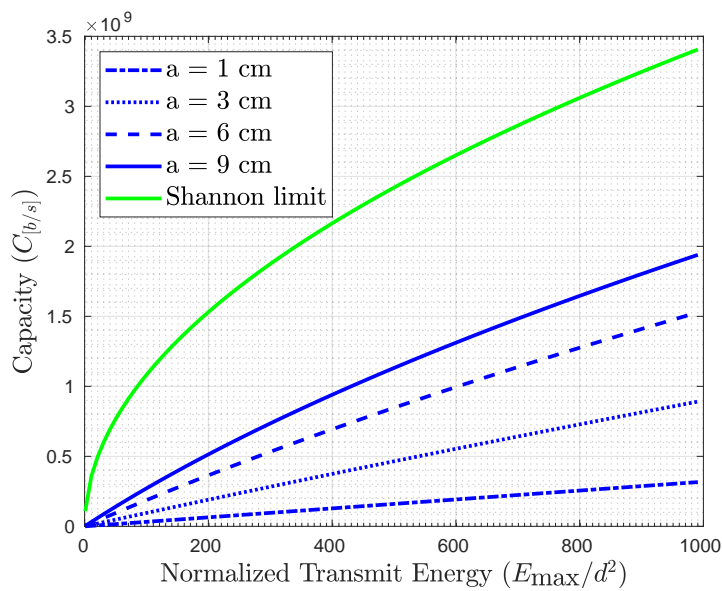


Fig. 8: Achievable rates for four different antenna sizes as well as the Shannon limit as a function of the normalized transmit power density.

Next, we focus on the interference scenario and investigate the impact of the antenna size and the matching network on the mutual information. The interference power is set to the same value as transmit power (i.e $P_t = E_{\max} = 1.84 \times 10^{-8}$ Joules) and the interference pathloss exponent is chosen as $\alpha = 2.5$. We choose the distance between transmitter and receiver to be $d = R/3$. Our approach is to compare the following two achievable rate ratios: i) $C_{\text{inter}}^{\text{no MN}}/C_{\text{Shannon}}$ which

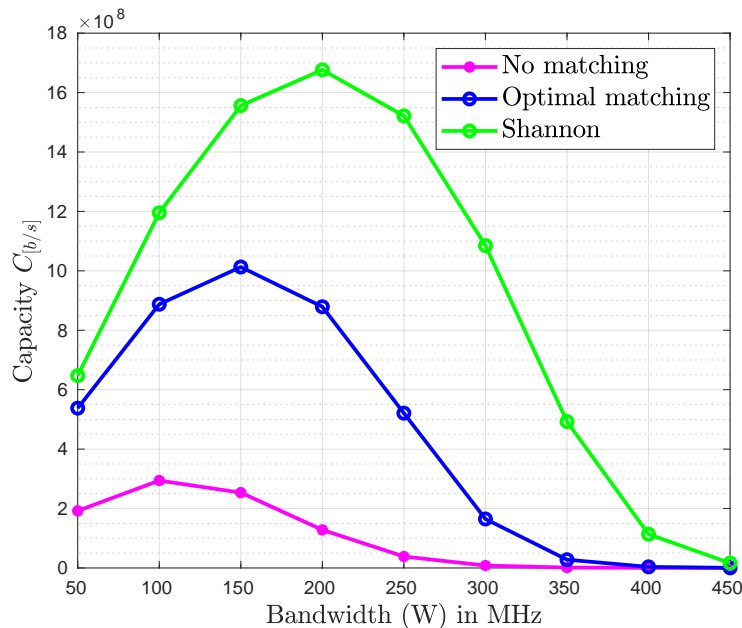


Fig. 9: Capacity vs. Bandwidth for a fixed antenna size $a = 0.96$ cm.

represents the fraction of capacity achieved when no impedance matching is considered, and ii) $C_{\text{inter}}^{\text{MN}}/C_{\text{Shannon}}$ corresponding to the equivalent capacity fraction when the matching network is part of the SISO communication model. Fig. 10 depicts how these two ratios increase as function of the user density ρ for two different antenna sizes. There, we see that the proposed closed-form approximation (46) of $C_{\text{inter}}^{\text{no MN}}$ has a second-order truncation error that is rather small for this case with interference pathloss $\alpha = 2.5$ (but might be loose for higher α). By varying the user density $\rho = 1/(\pi R^2)$ (in users per m^2) as a function of the cell radius R , it is seen that these ratios approach 1 with higher network densification, and reach the interference-limited regime (i.e. the achievable rate plateau) starting from a user density that depends on the presence or absence of the matching network. In this interference-limited regime, it is interesting to notice that the achievable rate is not dependent on the antenna size, as both interference and intended signal are undergoing the same antenna frequency response regardless of the antenna size.

Confirmed by Fig. 10 and the previous results, we can conclude that future wireless networks open up new research directions for the antenna design, where information-theoretic design criteria might be more appropriate than conventional antenna design practices. In particular, antenna directivity becomes more critical than antenna matching efficiency in interference-limited networks, which requires understanding such trade-offs on a unified theoretical level.

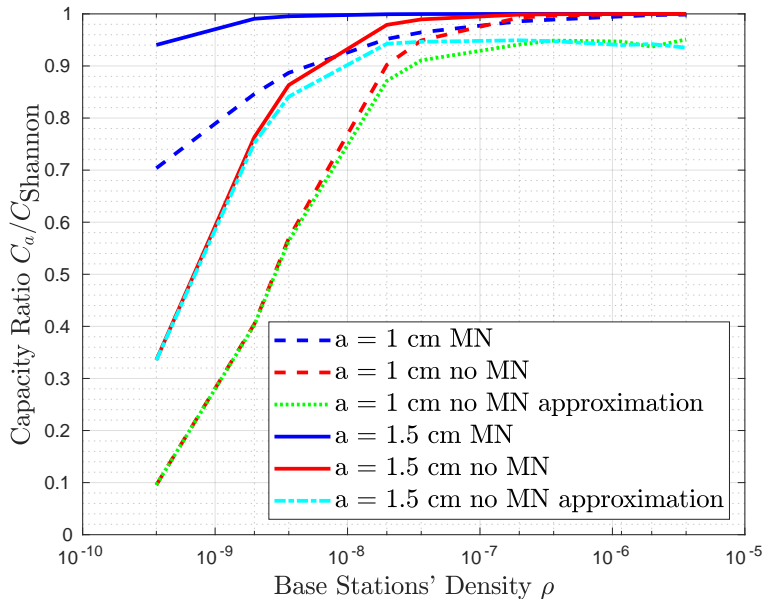


Fig. 10: Achievable rate ratio vs. Base stations' density ρ for a two antenna sizes $a = 1$ cm and $a = 1.5$ cm with $\alpha = 2.5$.

VI. CONCLUSION

In this paper, we established the mutual information of a SISO wireless channel with the constraint on the antenna size at the receiver. After developing a circuit theoretic channel model, we computed the maximum mutual information per unit time between the input and output of a circuit system. Chu and Bode/Fano theories [14], [16] were used to incorporate the size constraints. Our investigation revealed that the mutual information, specifically in the low SNR regime, is severely degraded by the finite-size constraint. The optimal signaling bandwidth was further determined to be a significant fraction of the carrier showing that broadband communication systems are possible with compact antennas. Finally, when interference was considered, we showed how the antenna size affects the mutual information only in the noise-limited regime, unlike the interference-limited region where the antenna size is immaterial. Additional adaptations, tests, and experiments have been left for a future work in which a generalization to multiple antennas and/or users can be considered. As a future direction, it is important to consider the design of broadband antennas to approach the derived mutual information. Practically, relevant problems of establishing the achievable data rate of some common types of antennas (e.g. dipole, monopole, horn, aperture) are also interesting directions for future work.

APPENDIX I

DERIVATION OF BROADBAND MATCHING CONSTRAINTS

In this appendix, based on the conditions of physical realizability of the reflection coefficient from [14], we derive the integral constraints in (8) and (9). It was shown by Darlington in [28] that any physically realizable impedance can be regarded as an input impedance of a reactive two-port network that is terminated with a resistance R . For better illustration, the Darlington representation of the Chu-equivalent impedance is boxed in Fig. 3. Without loss of generality, the resistance R_2 can be taken to be equal to $1\ \Omega$. To find the integral constraints, it is first required to determine the zeros of the transmission coefficient of Darlington network terminated with $1\ \Omega$ resistance as depicted in Fig. 11. Using the Laplace transform, the transmission coefficient defined as:

$$T(s) = \frac{2V_1}{E_1}, \quad (50)$$

can be found to be

$$T(s) = \frac{2s^2 \frac{a^2}{c^2}}{2s^2 \frac{a^2}{c^2} + 2s \frac{a}{c} + 1}. \quad (51)$$

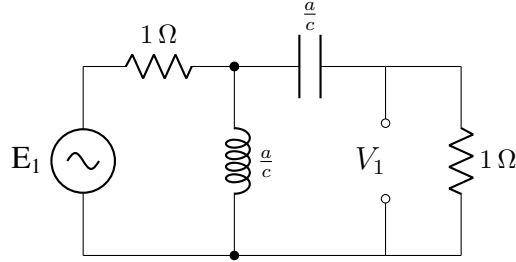


Fig. 11: Darlington reactive network transmission coefficient

From [14], the two zeros of the transmission coefficient at the origin result in two integral constraints of the form:

$$\frac{1}{2\pi^2} \int_0^\infty f^{-2} \ln \left(\frac{1}{|\Gamma(f)|^2} \right) df = A_0^1 - 2\gamma^{-1}, \quad (52)$$

and

$$\frac{1}{8\pi^4} \int_0^\infty f^{-4} \ln \left(\frac{1}{|\Gamma(f)|^2} \right) df = -A_0^3 + \frac{2}{3}\gamma^{-3}. \quad (53)$$

where A_0^1 and A_0^3 have to be determined from the reflection coefficient of the Darlington-equivalent network terminated with $1\ \Omega$ resistance. This corresponds to finding the reflection

coefficient from the input impedance in Fig. 2 when setting $R_2 = 1$. The reflection coefficient is given by:

$$\Gamma(s) = \frac{1}{2s^2 \frac{a^2}{c^2} + 2s \frac{a}{c} + 1}. \quad (54)$$

Moreover, the coefficients A_0^1 and A_0^3 are then given by:

$$A_0^1 = \left. \frac{d}{ds} \ln \left(\frac{1}{\Gamma(s)} \right) \right|_{s=0} = \frac{2a}{c}, \quad (55)$$

and

$$A_0^3 = \left. \frac{1}{6} \frac{d^3}{ds^3} \ln \left(\frac{1}{\Gamma(s)} \right) \right|_{s=0} = -\frac{4a^3}{3c^3} \quad (56)$$

thereby yielding to the expressions in (8) and (9).

APPENDIX II

RADIATED EM FIELDS OF CHU'S ANTENNAS AND THEIR EQUIVALENT CIRCUIT

We review in this appendix the general form of the radiated electromagnetic fields of a Chu's antenna of size a in terms of radiation modes and their equivalent input impedance. Consider an antenna structure that is completely embedded inside a geometrical spherical volume of radius a . Using the following definitions,

- $P_n(\cos \theta)$ the Legendre polynomial of order n ,
- $P_n^1(\cos \theta)$ associated Legendre polynomial of first kind,
- $h_n(kr)$ the spherical Hankel function of the second kind,
- $k = \omega \sqrt{\epsilon \mu} = \frac{2\pi}{\lambda}$ the wave number,
- $\sqrt{\frac{\mu}{\epsilon}}$ the wave impedance of a plane wave in free space, and
- $\{A\}_n$ complex coefficients specified by the radiation characteristics.

For a vertically polarized antenna the three components of EM fields outside the sphere in the spherical coordinate system, (r, θ, ϕ) , are given in [16] by

$$H_\phi = \sum_{\substack{n=1 \\ n \text{ odd}}}^{\infty} A_n P_n^1(\cos \theta) h_n(kr), \quad (57a)$$

$$E_r = -j \sqrt{\frac{\mu}{\epsilon}} \sum_{\substack{n=1 \\ n \text{ odd}}}^{\infty} A_n n(n+1) P_n(\cos \theta) \frac{h_n(kr)}{kr}, \quad (57b)$$

$$E_\theta = j \sqrt{\frac{\mu}{\epsilon}} \sum_{\substack{n=1 \\ n \text{ odd}}}^{\infty} A_n P_n^1(\cos \theta) \frac{1}{kr} \frac{\partial}{\partial r} (r h_n(kr)). \quad (57c)$$

These EM fields are expressed in terms of a sum of a set of orthogonal spherical waves, propagating outward the sphere. Each term in these sums contributes to a “*radiation mode*” weighted by a coefficient A_n . For a given antenna structure and current distribution, the set of coefficients, A_n , could be obtained from boundary conditions at the surface of the structure. In [16], by leaving the set of coefficients unspecified, Chu converted the electromagnetic radiation problem to an equivalent circuit problem by deriving an equivalent circuit model for each of the TM_n waves based on the complex power calculation [16]. Indeed by integrating the complex Poynting vector, $\mathbf{S} = \mathbf{E} \times \mathbf{H}^*$, over the hypothetical sphere of radius a , the total complex power stored in the electromagnetic field outside the spherical structure is

$$\begin{aligned} P(a) &= \int_{\text{sphere}} \mathbf{S} \cdot d\mathbf{S} = \int_0^{2\pi} \int_0^\pi E_\theta H_\phi a^2 \sin\theta d\theta d\phi \\ &= j 2\pi \sqrt{\frac{\mu}{\epsilon}} \sum_{\substack{n=1 \\ n \text{ odd}}}^{\infty} \left(\frac{A_n}{k}\right)^2 \frac{n(n+1)}{2n+1} \rho h_n(\rho) \frac{\partial}{\partial \rho} \left(\rho h_n(\rho)\right), \end{aligned} \quad (58)$$

in which $\rho = ka$. Due to orthogonality of Legendre polynomials, the total complex power is given as a sum of complex powers for each spherical wave. It is seen from (58) that the n^{th} term in the sum is equivalent to the complex power in a circuit with the voltage and current being given by

$$V_n = j \sqrt[4]{\frac{\mu}{\epsilon}} \frac{A_n}{k} \sqrt{\frac{4\pi n(n+1)}{2n+1}} \frac{\partial}{\partial \rho} \left(\rho h_n(\rho)\right), \quad (59a)$$

$$I_n = \sqrt[4]{\frac{\mu}{\epsilon}} \frac{A_n}{k} \sqrt{\frac{4\pi n(n+1)}{2n+1}} \rho h_n(\rho), \quad (59b)$$

from which the impedance can be obtained as the ratio:

$$Z_n = \frac{V_n}{I_n} = j \frac{\frac{\partial}{\partial \rho} (\rho h_n(\rho))}{\rho h_n}. \quad (60)$$

By letting $n = 1$, we recover the circuit characteristics of the electric Chu’s antenna (4). From the expression of Z_n , an equivalent circuit for TM_n wave can be obtained based on the recursion formula for spherical Bessel functions [16]. The equivalent circuit has a ladder structure with series capacitances and shunt inductances with a single dissipate element at the end. Higher-order modes store a large amount of electromagnetic energy in the fields and can have more directivity gain at the expense of bandwidth.

REFERENCES

- [1] C. E. Shannon, "A mathematical theory of communication," *Bell system technical journal*, vol. 27, no. 3, pp. 379–423, 1948.
- [2] M. Franceschetti, *Wave theory of information*. Cambridge University Press, 2017.
- [3] F. K. Gruber and E. A. Marengo, "New aspects of electromagnetic information theory for wireless and antenna systems," *IEEE Transactions on Antennas and Propagation*, vol. 56, no. 11, pp. 3470–3484, 2008.
- [4] M. D. Migliore, "On electromagnetics and information theory," *IEEE Transactions on Antennas and Propagation*, vol. 56, no. 10, pp. 3188–3200, 2008.
- [5] M. T. Ivrlač and J. A. Nossek, "Toward a circuit theory of communication," *IEEE Transactions on Circuits and Systems I: Regular Papers*, vol. 57, no. 7, pp. 1663–1683, 2010.
- [6] J. W. Wallace and M. A. Jensen, "Mutual coupling in MIMO wireless systems: A rigorous network theory analysis," *IEEE Transactions on Wireless Communications*, vol. 3, no. 4, pp. 1317–1325, 2004.
- [7] R. W. Heath Jr and A. Lozano, *Foundations of MIMO communication*. Cambridge University Press, 2018.
- [8] T. L. Marzetta, "Noncooperative cellular wireless with unlimited numbers of base station antennas," *IEEE Transactions on Wireless Communications*, vol. 9, no. 11, pp. 3590–3600, 2010.
- [9] K.-L. Wong, *Compact and broadband microstrip antennas*. John Wiley & Sons, 2004, vol. 168.
- [10] J. L. Massey, "Applied digital information theory," *lecture notes, ETH Zurich*. [Online]. Available: http://www.isiweb.ee.ethz.ch/archive/massey_scr/adit1.pdf, 1998.
- [11] P. S. Taluja and B. L. Hughes, "Information theoretic optimal broadband matching for communication systems," in *2010 IEEE Global Telecommunications Conference GLOBECOM 2010*. IEEE, 2010, pp. 1–6.
- [12] A. Mezghani and R. W. Heath, "The information and wave-theoretic limits of analog beamforming," in *2018 Information Theory and Applications Workshop (ITA)*. IEEE, 2018, pp. 1–6.
- [13] S. Saab, A. Mezghani, and R. W. Heath, "Capacity based analysis of a wideband simo system in the presence of mutual coupling," in *2019 IEEE Global Communications Conference (GLOBECOM)*. IEEE, 2019, pp. 1–6.
- [14] R. M. Fano, "Theoretical limitations on the broadband matching of arbitrary impedances," *Journal of the Franklin Institute*, vol. 249, no. 1, pp. 57–83, 1950.
- [15] M. Gustafsson and S. Nordebo, "On the spectral efficiency of a sphere," *Progress In Electromagnetics Research*, vol. 67, pp. 275–296, 2007.
- [16] L. J. Chu, "Physical limitations of omni-directional antennas," *Journal of applied physics*, vol. 19, no. 12, pp. 1163–1175, 1948.
- [17] H. Bode, "A method of impedance correction," *Bell System Technical Journal*, vol. 9, no. 4, pp. 794–835, 1930.
- [18] R. G. Gallager, *Information theory and reliable communication*. Springer, 1968, vol. 2.
- [19] R. C. Hansen and R. E. Collin, *Small antenna handbook*. John Wiley & Sons, 2011.
- [20] A. S. Sedra, D. E. A. S. Sedra, K. C. Smith, and K. C. Smith, *Microelectronic circuits*. Oxford University Press, 1998.
- [21] H. Nyquist, "Thermal agitation of electric charge in conductors," *Physical review*, vol. 32, no. 1, p. 110, 1928.
- [22] I. M. Gel'fand and A. M. Yaglom, "Computation of the amount of information about a stochastic function contained in another such function," *Uspekhi Matematicheskikh Nauk*, vol. 12, no. 1, pp. 3–52, 1957.
- [23] R. F. Harrington, *Time-Harmonic Electromagnetic Fields*. McGraw-Hill, 1961.
- [24] R. W. Heath, M. Kountouris, and T. Bai, "Modeling heterogeneous network interference using poisson point processes," *IEEE Transactions on Signal Processing*, vol. 61, no. 16, pp. 4114–4126, 2013.

- [25] S. Akoum and R. W. Heath, "Interference coordination: Random clustering and adaptive limited feedback," *IEEE Transactions on Signal Processing*, vol. 61, no. 7, pp. 1822–1834, 2013.
- [26] "stochastic geometry and wireless networks: Volume i theory," *Foundations and Trends in Networking*, vol. 3, 2010. [Online]. Available: <http://dx.doi.org/10.1561/13000000006>
- [27] R. W. Heath Jr, T. Wu, Y. H. Kwon, and A. C. Soong, "Multiuser MIMO in distributed antenna systems with out-of-cell interference," *IEEE Transactions on Signal Processing*, vol. 59, no. 10, pp. 4885–4899, 2011.
- [28] S. Darlington, "Synthesis of reactance 4-poles which produce prescribed insertion loss characteristics: Including special applications to filter design," *Journal of Mathematics and Physics*, vol. 18, no. 1-4, pp. 257–353, 1939.